

Validation of a simulation model in TRNSYS for an institutional photovoltaic system: Case study at the University of Santander - UDES

F. Gomez¹, B. E. Tarazona-Romero², J. G. Ascanio-Villabona², O. Palomino-Prieto^{1,2}, N. Y. Castillo-Leon², N. D. Socha-Rojas³

¹ Universidad de Santander UDES. Bucaramanga, Santander 680005, Colombia

² Unidades Tecnológicas de Santander UTS. Bucaramanga, Santander 680005, Colombia

³ Universidad Industrial de Santander UIS. Bucaramanga, Santander 680005, Colombia

*Corresponding author E-mail: btarazona@correo.uts.edu.co

ABSTRACT

The objective of this study is to develop and validate an energy simulation model in TRNSYS to evaluate the performance of the grid-connected photovoltaic system installed in the Guane building of the University of Santander (UDES), located in Bucaramanga, Colombia. A technical characterization of the system was performed, followed by the design of a model in TRNSYS using real configuration, operational, and meteorological data. Subsequently, an experimental validation was carried out based on the comparison between simulated values and measured data during the year 2024, using statistical metrics such as absolute error, relative error, and accuracy. The model achieved an average relative error of 3.3%, with an average absolute difference of 146.47 W, demonstrating an overall agreement of more than 96% between simulated and experimental results. These results show that the model reproduces, with high fidelity, the behavior of the photovoltaic system under real conditions. The validated model represents a useful tool for energy management, maintenance planning, and operational optimization of institutional solar systems, and it is replicable in similar tropical contexts. In addition, it enables the exploration of expansion scenarios and sustainable energy transitions from both academic and technical perspectives.

Keywords:

Energy Simulation, Photovoltaic System, TRNSYS, Validation.

1. Introduction

The global energy transition has driven the adoption of renewable sources as a response to climate change [1] and the need to reduce dependence on fossil fuels. In this context, photovoltaic (PV) systems have established themselves as an effective alternative for distributed energy generation, especially in the institutional and academic setting [2]. Universities and research centers have implemented these technologies not only as an energy solution, but also as platforms for teaching, analysis, and experimentation. In Colombia, this trend has gained momentum due to the legal framework established by Law 1715 of 2014, which encourages the use of non-conventional energy sources (FNCE) and promotes the integration of modeling tools for their efficient management [3].

In this context, TRNSYS (Transient System Simulation Tool) has become one of the most robust and versatile computational tools for energy simulation [4]. Its ability to dynamically represent thermal and electrical systems under real conditions [5] has been widely validated by the scientific community [6]. Several studies have demonstrated its effectiveness for modeling PV configurations in residential [7], commercial and institutional buildings [8], as well as for evaluating storage strategies [9], smart grid integration [10] and energy efficiency analysis [11]. Empirical validation of these models is key to their practical application in real projects.

Recent research has focused its efforts on validating PV models using experimental data in order to reduce prediction errors and increase reliability in operational decision making [12]. These validations allow detecting unmodeled losses, adjusting thermal coefficients [13], and simulating alternative configurations that could optimize system performance [14]. However, despite the growth in the adoption of TRNSYS in academic

institutions, there are important gaps in the specific validation of systems installed in tropical contexts and in institutional buildings such as those of the University of Santander (UDES), which represents a significant opportunity for applied research.

This document is structured in four main sections. The first section corresponds to the Introduction, where the context, the problem, the hypothesis and the objectives of the study are presented. The second section develops the Methodology, detailing the research design, the characterization of the photovoltaic system and the construction of the model in TRNSYS. The third section presents the Results and Discussion, in which the simulation data, the model validation process and the comparative analysis with the experimental values are presented. Finally, the fourth section is dedicated to the Conclusions, where the main findings are synthesized, the fulfillment of the objectives is evaluated and future lines of research oriented to the optimization and expansion of the validated model are proposed.

2. Methods and Materials

2.1. Photovoltaic system

The photovoltaic system to be modeled is located on the terraces of the Guane buildings, within the facilities of the University of Santander (UDES), in the municipality of Bucaramanga, Colombia. The geographical location of the system corresponds to the coordinates $7^{\circ} 6' 21.00''$ north latitude and $73^{\circ} 5' 42.28''$ west longitude, equivalent to planar coordinates 7.105834 latitude and -73.09506 longitude.

The solar energy system installed on the roof of the Guane Building at the University of Santander (UDES) has a nominal capacity of 30.7 kWp and is designed to operate in an ON-GRID configuration, with an estimated annual production of 47.78 MWh. It consists of 96 Up Solar model UP-M320M photovoltaic modules, each rated at 320 Wp with an efficiency of 16.5%, distributed across six parallel strings with 16 panels in series per string. These are organized into two MPPT banks connected to a central inverter, ABB model TRIO 27.6 TL OUTD-S2X-400/JP, with a nominal power of 27.6 kW and an efficiency of 98.2%.

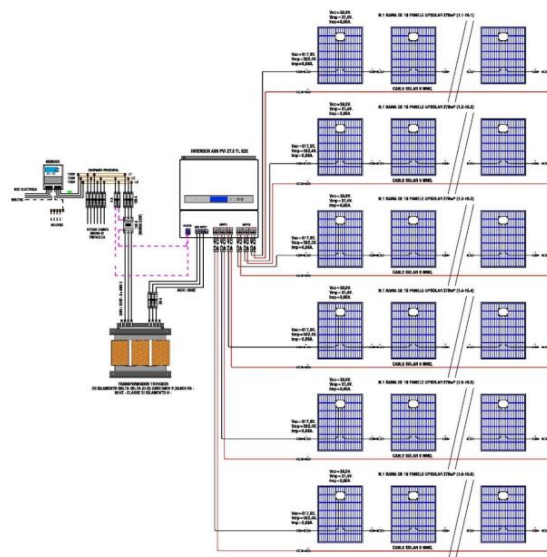


Figure 1. Planimetry of connection in the Guane-UDES Building [15]

The panels were installed at an inclination of 10° , selected to maximize solar radiation collection based on the site's latitude and local climatic conditions. The total surface area occupied by the modules is 177 m^2 , with an operating voltage of 547 V and a maximum current of 51 A. This configuration enables efficient maximum power point tracking (MPPT) and ensures optimal performance throughout the year. Figure 1 shows the system's installation plan on the roof of the Guane Building, illustrating a layout free from shadows and obstructions—ideal for solar energy utilization.

2.2. Mathematical Models

The Type 194 component of TRNSYS was selected for its ability to implement the five-parameter model proposed by [16], which enables the estimation of the electrical performance of a grid-connected PV system. This model calculates the current and power of the PV array at a given voltage, as well as the corresponding values at the maximum power point (MPP). Its main advantage lies in the ability to extrapolate manufacturer-

provided data under standard test conditions (1,000 W/m², 25 °C) to various real operating scenarios, which is essential for simulating specific configurations and optimizing system performance. The representation of this model is based on an equivalent circuit, as illustrated in Figure 2.

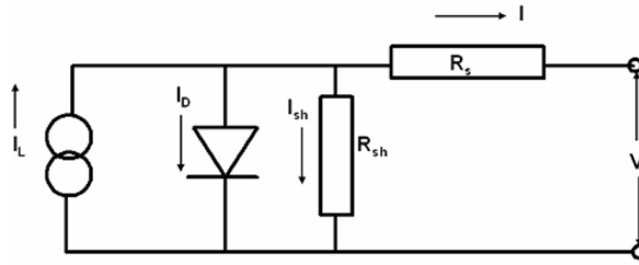


Figure 2. Electrical diagram of the mathematical model [16]

The current–voltage (I–V) characteristics of a photovoltaic array vary depending on the solar irradiance and temperature conditions to which it is exposed. The photovoltaic (PV) model enables the determination of the I–V curve under these environmental conditions by using five matrices derived from the nominal specifications provided by the manufacturer. The mathematical relationship that describes the current and voltage of the circuit shown in Figure 2 is given by the following equation:

$$I = I_L - I_0 \left(e^{\frac{V + Ir_s}{a}} - 1 \right) + \frac{V + Ir_s}{R_{sh}} \quad (1)$$

Where,

$$a = \frac{n_s * n_i * K * T_c}{q} \quad (2)$$

It is important to note that, in order to determine the current, voltage, and consequently the power delivered to the load, five fundamental parameters must be known: the light-generated current (I_L), the diode reverse saturation current (I_0), the series resistance (R_s), the shunt resistance (R_{sh}), and the diode ideality factor (n). The series resistance (R_s), shunt resistance (R_{sh}), and the modified ideality factor (a) are defined in Equation (2). To accurately evaluate the five parameters in Equation (1), five independent data points are required. These parameters are directly influenced by the incident solar irradiance on the PV array and its operating temperature.

The reference values for these parameters are established under standard rating conditions (SRC), typically defined as an irradiance of 1,000 W/m² and a temperature of 25 °C. Manufacturers generally provide three sets of current–voltage data under these conditions: the short-circuit current (I_{sc}), the open-circuit voltage (V_{oc}), and the current and voltage at the maximum power point (I_{mp} , V_{mp}).

Additionally, a fourth data point is obtained by recognizing that the derivative of power with respect to voltage is zero at the maximum power point (P_{mp}). Although both the open-circuit voltage temperature coefficient (βV_{oc}) and the short-circuit current temperature coefficient (αI_{sc}) are known, only βV_{oc} is used to determine the five reference parameters. In contrast, αI_{sc} is applied when the cell operates under conditions different from the standard reference.

The five parameters in Equation (1), corresponding to operation under standard rating conditions (SRC), are denoted as a_{ref} , $I_{0,ref}$, $I_{L,ref}$, $R_{s,ref}$, and $R_{sh,ref}$. To determine these reference values, the three known current–voltage pairs (I–V) under SRC are substituted into Equation (1), resulting in a system of equations described by Equations (3) through (5). For the short-circuit condition, the current is set as $I = I_{sc,ref}$ and the voltage as $V = 0$.

$$I_{sc,ref} = I_{L,ref} - I_{0,ref} \left(e^{\frac{I_{sc,ref} R_{s,ref}}{a_{ref}}} - 1 \right) - \frac{I_{sc,ref} R_{s,ref}}{R_{sh,ref}} \quad (3)$$

For the maximum power point, $I=0$, $V= V_{sc,ref}$

$$0 = I_{L,ref} - I_{o,ref} \left(e^{\frac{V_{oc,ref}}{a_{ref}}} - 1 \right) - \frac{V_{oc,ref}}{R_{sh,ref}} \quad (4)$$

For the maximum power point, $I = I_{sc,ref}$, $V = V_{sc,ref}$

$$I_{mp,ref} = I_{L,ref} - I_{o,ref} \left(e^{\frac{V_{mp,ref} + I_{mp,ref} R_{s,ref}}{a_{ref}}} - 1 \right) - \frac{V_{mp,ref} + I_{mp,ref} R_{s,ref}}{R_{sh,ref}} \quad (5)$$

The temperature coefficient of the open circuit voltage is given by:

$$\mu Voc = \frac{\partial V}{\partial T} \Big|_{I=1} \approx \frac{V_{oc,ref} - V_{oc,Tc}}{T_{ref} - T_c} \quad (6)$$

To numerically calculate the open-circuit voltage temperature coefficient (μVoc), it is necessary to know the value of Voc at a temperature close to the reference temperature (T_{ref}), although variations of up to ± 10 K do not significantly affect the result. This value can be determined using the appropriate equation, provided that the temperature dependence expressions for the parameters I_o , I_L , and a are available, assuming that the shunt resistance (R_{sh}) remains constant with temperature.

Furthermore, TRNSYS employs a unit conversion model that enables input variables—such as temperature in degrees Celsius ($^{\circ}C$)—to be transformed into other required units (e.g., $^{\circ}F$) using multiplication and addition factors defined in configuration files. This process ensures consistency across system calculations by validating input types and units, applying standardized conversion expressions, and facilitating their integration into other components of the model.

$$X_{st} = \frac{X_i - a_i}{m_i} \quad (7)$$

The desired output units specifier ($V_{out,i}$) is then read, and the corresponding multiplication (m_o) and addition (a_o) factors are retrieved from the *Units.lab* file. Finally, the conversion from standard units to the desired output units is performed using the following expression:

$$Y_i = X_{st} * m_o + a_o \quad (8)$$

2.3. Simulation Modeling TRNSYS

In the proposed simulation, specific TRNSYS components are employed and organized into four main categories: (i) *inputs*, which include relevant meteorological parameters; (ii) *auxiliary components*, required for intermediate calculations; (iii) *main components*, which comprise the photovoltaic model with grid injection and the associated inverter; and (iv) *outputs*, representing the results obtained, such as generated power, current, and voltage.

The input components are further classified based on their function into: (i) *data readers* and (ii) *input conditioners*. Data readers enable the importation of information from external files, allowing the incorporation of meteorological data in various formats (see Figure 3). In this simulation, two data readers were used: one configured for reading meteorological files in TMY format, and another for reading *.txt* files during the validation phase. Note that Figure 3 does not include the *.txt* reader, as the preliminary simulation was conducted using average meteorological data for Bucaramanga, Colombia.

For auxiliary components, a unit converter was used in TRNSYS specifically for the temperature variable, ensuring consistency during the simulation by converting temperature data from Kelvin (K) to degrees Celsius ($^{\circ}C$). For the visualization and storage of generated data, a graphing and printing component was used to enable real-time monitoring and proper recording of results.

Finally, to ensure accuracy in the results, calculators were included to first account for inverter efficiency and subsequently estimate the system's output power. The final results were corrected according to this efficiency

factor, as the default TRNSYS model did not inherently account for inverter efficiency. Additionally, connections between the inputs and outputs of the Types were represented with color-coded lines, which facilitated the identification of each process variable throughout the simulation model.

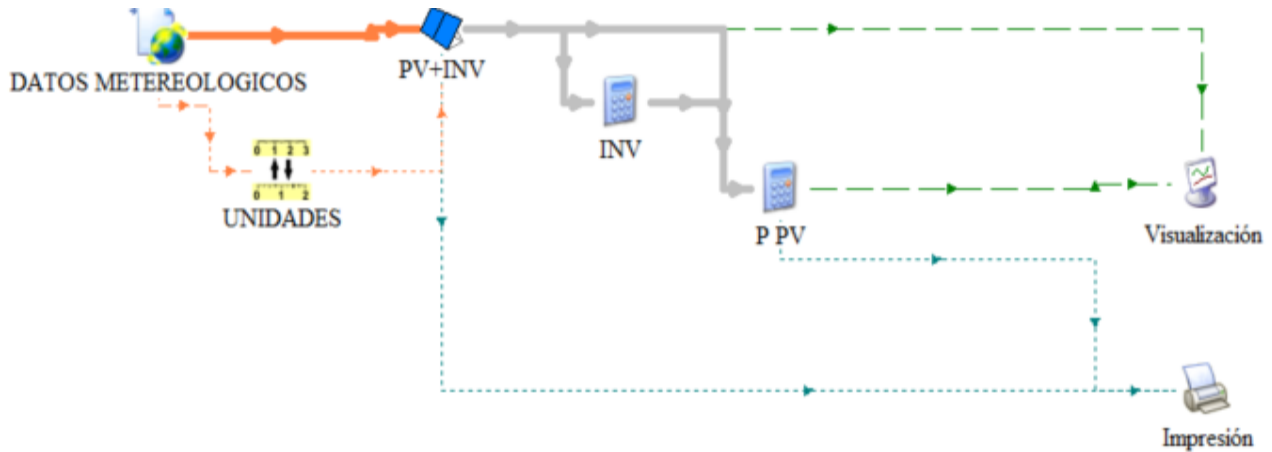


Figure 3. Simulation Model

2.4. Validation Method

The validation process of the proposed simulation model involves evaluating the results obtained using specific meteorological data and comparing them with the behavior recorded experimentally. This analysis enables the identification of potential discrepancies between the simulated performance and the real system's operation, with the aim of refining and improving the model's accuracy when necessary.

Model validation is carried out through a dual evaluation approach, combining qualitative and quantitative analyses. The qualitative analysis is based on the graphical representation of key variables—current, voltage, and power—allowing a visual comparison between the experimentally measured values and the predictions generated by the simulation model. This visual comparison helps assess the model's consistency and overall fidelity. The qualitative assessment is complemented by a quantitative analysis, which includes the estimation of absolute error, relative error, and maximum error to precisely quantify the model's accuracy.

The absolute error of a measurement (ε_a) is an indicator of the deviation present in a given measurement. It is calculated as the difference between the true (reference) value (X) and the measured value (X_i), as shown in Equation (9). The absolute error can be either positive or negative, depending on whether the measured value is greater or less than the actual value.

$$\varepsilon_a = (X) - (X_i) \quad (9)$$

The relative error (ε_r) is a percentage indicator of the accuracy of the measurement. It can be determined from the ratio of the absolute error (ε_a) to the mean value (X) (see Equation 10). Similar to the absolute error, the relative error can be either positive or negative, depending on the direction of the deviation.

$$\varepsilon_r = \frac{\varepsilon_a}{X} \cdot 100 \quad (10)$$

3. Results and discussion

3.1. Simulation Model

Figure 4 illustrates the variation in current (A) and power (W) over a full simulation year (8,736 hours), highlighting the typical behavior of a solar generation system, characterized by daily production cycles and periods of inactivity due to the absence of solar radiation. The current reaches a maximum value close to 50 A, while power peaks at approximately 6,000 W during optimal conditions. Throughout the year, sustained energy production is observed during a significant portion of the simulation period, allowing the estimation of an average annual power output between 3,000 and 3,500 W. This reflects the consistent and efficient performance of the system under variable environmental conditions.

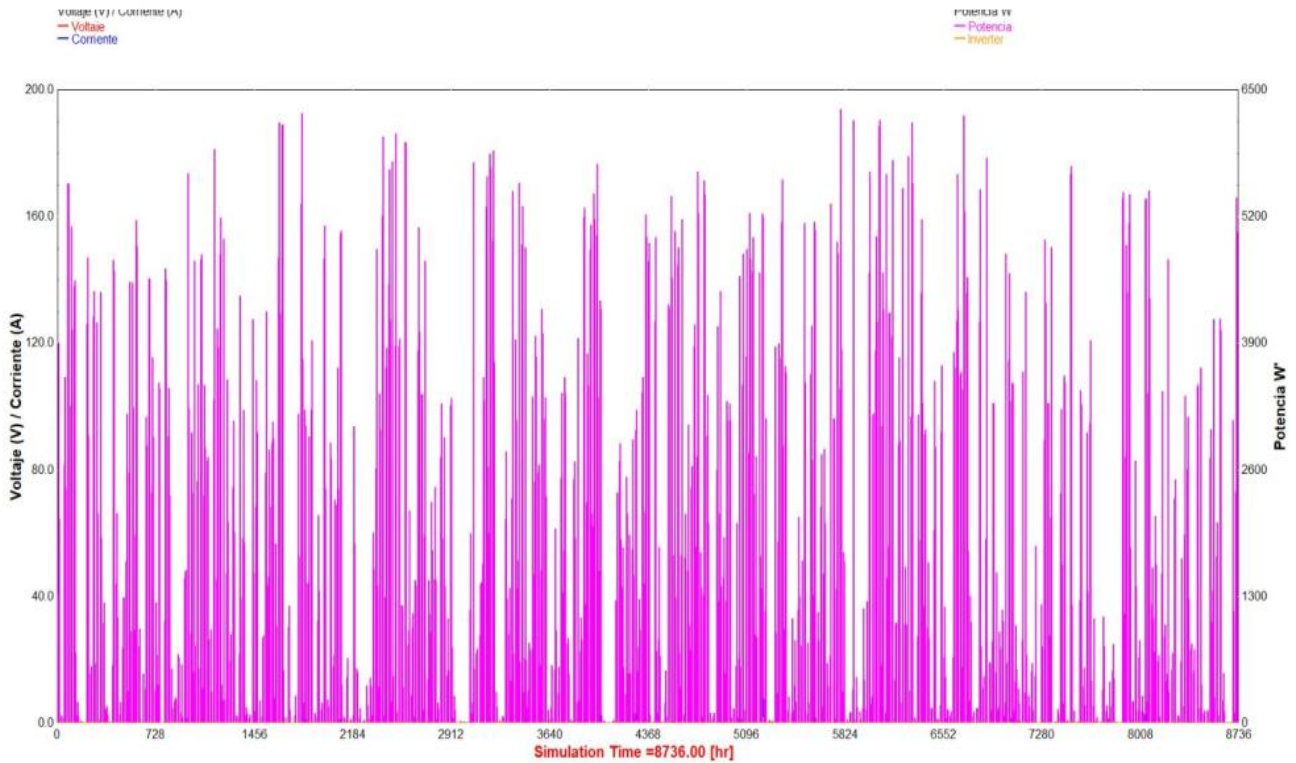


Figure 4. Model simulation in TRNSYS for 2023 meteorological data

3.2. Experimental Campaign

The experimental campaign supporting this project was conducted using data provided by the University of Santander (UNDES), which included key meteorological parameters such as ambient temperature, wind speed, and direct normal irradiation (DNI), recorded at defined intervals. Additionally, detailed electrical production data from the photovoltaic system—such as voltage, current, and generated power—were provided. This information was essential for comparing the simulation results with the actual system behavior, thereby ensuring a rigorous and consistent validation of the developed model.

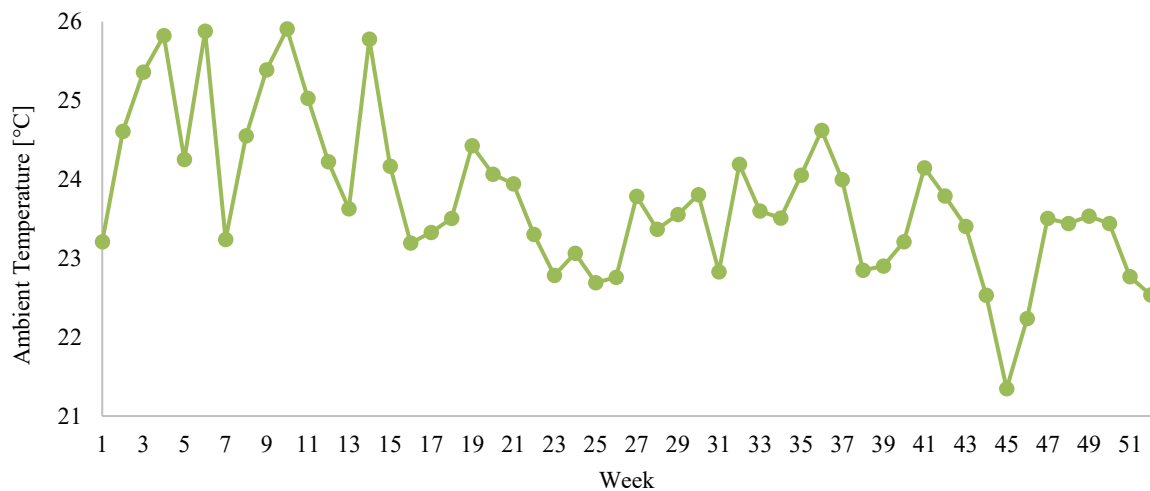


Figure 5. Weekly ambient temperature profiles in °C for the year 2024

The weekly ambient temperature profile throughout the year, presented in Figure 5, exhibits moderate fluctuations between 23 °C and 26 °C, reflecting the warm and stable climate of Bucaramanga. The highest temperatures occur during the initial weeks of the year, likely associated with increased solar radiation, while the lowest value, approximately 21.5 °C, is recorded around week 44. This thermal stability supports consistent operating conditions for solar systems, as ambient temperature directly influences the performance of photovoltaic panels and associated electronic devices, enabling efficient and predictable operation in tropical environments.

Figure 6 shows the weekly profile of average annual wind speed, measured in meters per second (m/s), over 52 weeks. A predominantly moderate trend is observed, with speeds ranging from 1.7 m/s to 3.2 m/s, and an isolated peak of 3.5 m/s occurring in week 24—the highest value of the year. During the first 13 weeks, wind speed exhibited greater variability, with several peaks exceeding 2.8 m/s, possibly influenced by seasonal factors. Between weeks 14 and 43, wind speed remained relatively stable, with values near or below 2 m/s, except for the aforementioned peak. In the final weeks of the year (weeks 45 to 52), a slight increase is observed, with values oscillating up to 2.5 m/s.

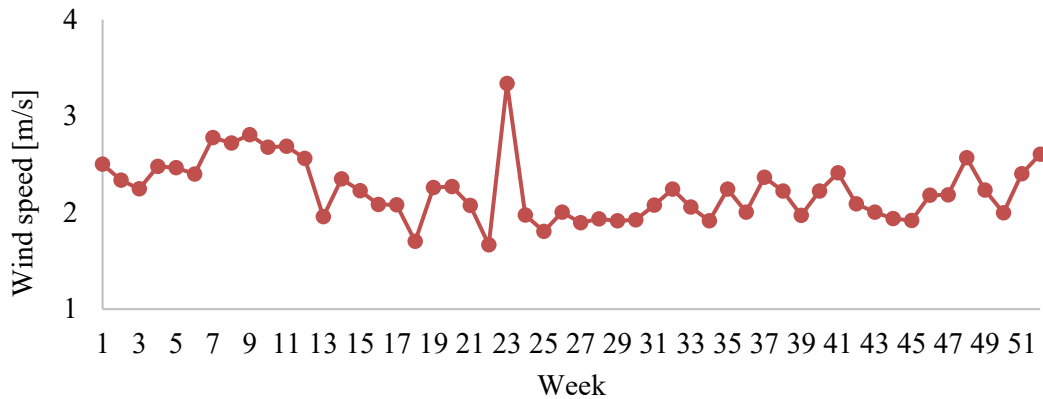


Figure 6. Weekly wind speed profiles (m/s) for the year 2024

Figure 7 presents the weekly profile of Direct Normal Irradiation (DNI) over the course of a year, with an annual average of 366.46 W/m² and notable weekly variability. The highest values are recorded between weeks 1 and 14, peaking at 468.85 W/m² in week 4, which highlights the strong solar capture potential during the first quarter of the year. A downward trend in irradiation is observed throughout the year, as indicated by a negative regression line, with the lowest value reaching 264.90 W/m² in week 45. Although a slight recovery is seen in the final quarter, the early-year peak values are not surpassed. This information is critical for the planning and design of solar energy systems, as it helps identify optimal collection periods and supports the development of backup strategies during months with lower solar availability.

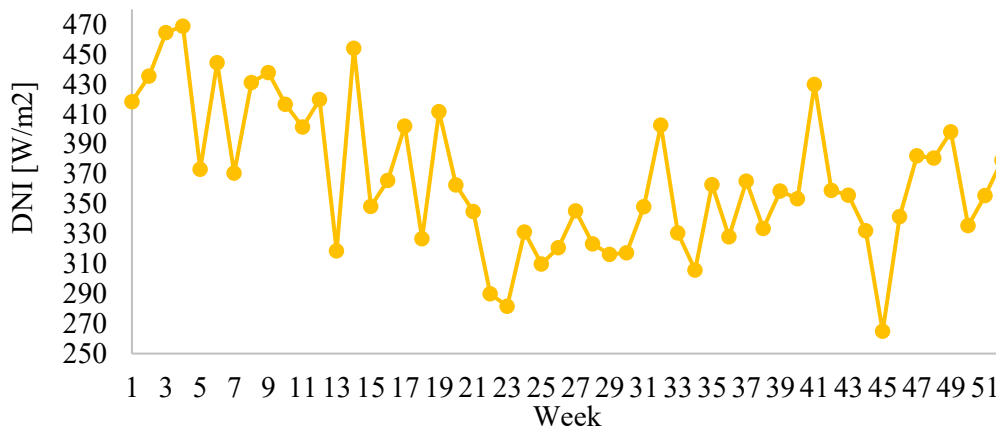


Figure 7. Weekly profiles of direct normal irradiation for the year 2024

During the 2024 experimental campaign, the system demonstrated consistent and significant energy production, with an average daily generation of 50.69 kWh (see Figure 8). The highest recorded value was 76.64 kWh, observed on April 10, likely due to optimal solar radiation conditions and favorable system performance. In contrast, the lowest value—31.70 kWh—occurred on April 4, possibly associated with adverse weather conditions such as dense cloud cover or rainfall. These data reflect natural variability, but within a range that supports the classification of the system as functionally stable and efficient.

The behavior of the generated energy suggests that the system responds effectively to environmental changes, maintaining daily production above 50 kWh on most days analyzed. This level of stability is critical for validation processes, as it confirms that the simulated outputs can be reliably compared with experimental data.

Moreover, having more than one-third of the days exceeding the average indicates a tangible potential to supply a significant portion of the daily energy demand of a medium-scale educational, residential, or commercial facility.

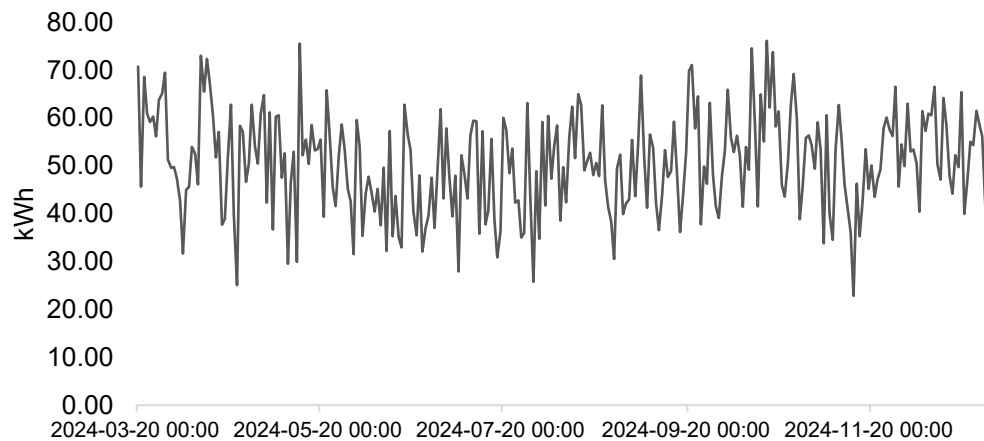


Figure 8. Electricity generation profile in kWh per day of the photovoltaic solar system implemented at UDES starting in March 2024

Regarding the average daily power, a mean value of 4,178.25 W was obtained, indicating that the system consistently delivers useful power during the active solar hours of the day. The maximum recorded value was 6,268.04 W, also observed on April 10, coinciding with the peak in energy generation and reinforcing the consistency of the system's behavior under high solar radiation conditions. The minimum value, 2,563.59 W, was recorded on April 4—the same day as the lowest energy output—further confirming the direct relationship between solar irradiance and photovoltaic system performance.

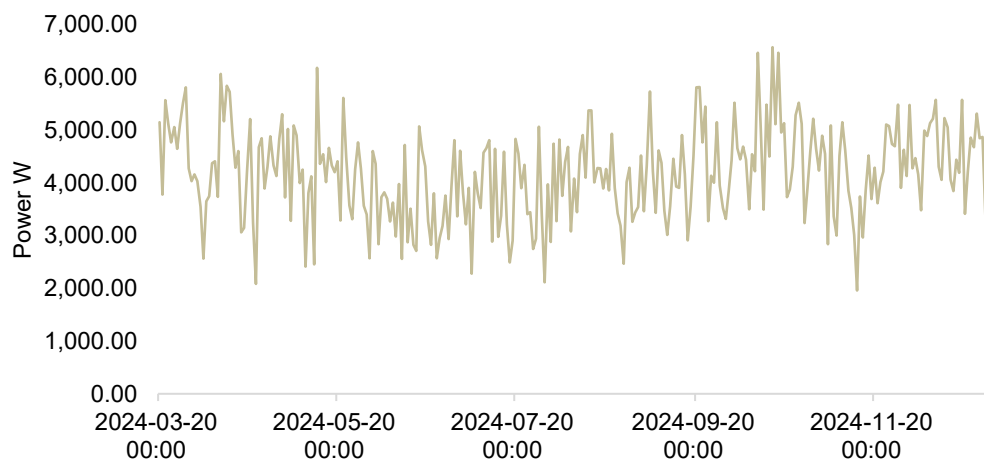


Figure 9. Profile of electrical power generated in W per day of the photovoltaic solar system implemented at UDES as of March 2024

This average power performance reflects appropriate system sizing and effective inverter operation, capable of sustaining moderate electrical loads for the majority of the day. An average power output of approximately 4 kW indicates that the system is not only operating correctly, but also has sufficient capacity to supply laboratory equipment, lighting systems, or even partially support institutional facilities. From a validation standpoint, these data serve as a critical reference point for comparison with simulation results, enabling parameter adjustments and confirming the reliability of numerical estimates against actual performance.

3.3. Validation

Figure 10 presents the comparison graph of simulated versus experimental power values, measured in watts. The results clearly show that the TRNSYS model accurately simulates the energy production of the photovoltaic system. The overall simulated weekly average power was 4,044.22 W, closely matching the on-site measured average of 4,190.69 W. This results in an average absolute difference of approximately 146.47 W,

corresponding to an average relative error of 3.3%, taking the measured power as the reference. In other words, the model underestimates the actual generation by only 3.3% on average, indicating minimal bias and excellent overall agreement. The small magnitude of this average error suggests that the model effectively captures the key factors influencing photovoltaic system performance, reflecting realistic behavior and proper parameter calibration.

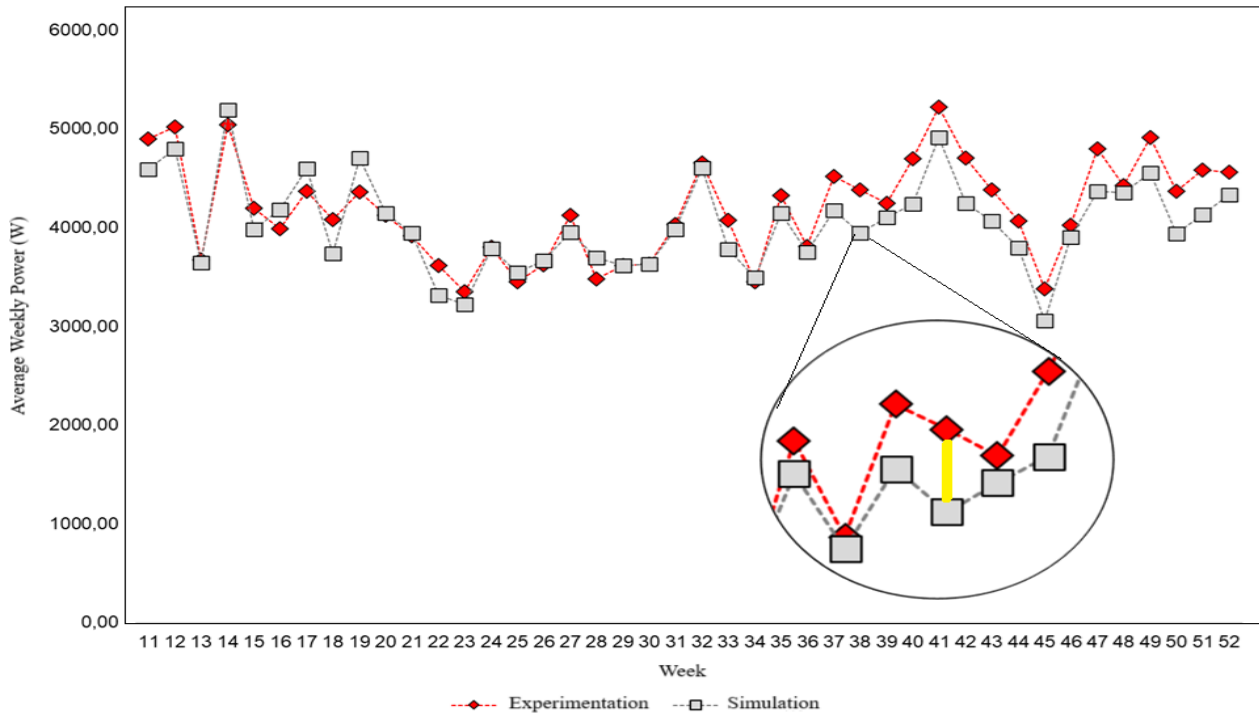


Figure 10. Simulation model validation graph

In addition, a week-by-week analysis was conducted to assess error variability and identify extreme deviation cases. The maximum absolute error observed was 458.03 W, corresponding to a maximum relative error of 10.01%. This indicates that, during the most divergent week, actual power generation exceeded the simulated output by approximately 10%, which is precisely at the upper threshold defined by the validation criterion (relative error $\leq 10\%$). Conversely, the minimum absolute error was -346.19 W, equivalent to a relative error of -7.94% , reflecting a scenario in which the model overestimated actual production by around 8% in a given week. In most cases, however, weekly deviations remained well below these extremes, falling within acceptable and consistent error margins.

Overall, the evaluation of these metrics confirms the satisfactory performance of the model and its compliance with the proposed validation criteria. An average relative error of 3.3% is notably low for this type of simulation study, demonstrating the high accuracy of the TRNSYS model in representing the real photovoltaic system. Moreover, the fact that nearly all weekly errors remained below the 10% threshold—with only one instance marginally exceeding it—further supports the model's reliability. Minor discrepancies may be attributed to external variables not fully captured by the simulation, such as short-term environmental fluctuations, slight measurement uncertainties, or inherent simplifications in component modeling. Despite these limitations, the model successfully replicates both the trend and magnitude of the system's energy output. In conclusion, given the low observed error rates and full adherence to the established validation threshold (relative error $< 10\%$), the TRNSYS model is considered validated and reliable for predicting the energy behavior of the Guane Building photovoltaic system with a high degree of confidence.

4. Conclusions

The simulation model developed in TRNSYS was successfully validated using experimental data from 2024, achieving an average accuracy of 96.7% in estimating the weekly generated power. The model exhibited an average relative error of only 3.3% and an average absolute error of 146.47 W, fully meeting the accuracy criterion established in the initial hypothesis (relative error $< 10\%$). These results validate the model's capability to represent the real behavior of an institutional photovoltaic system operating in a tropical Andean climate, confirming its applicability in similar energy analysis scenarios.

The experimentally recorded average power (4,190.69 W) and the simulated average (4,044.22 W) revealed a minimal discrepancy, indicating accurate system characterization and appropriate parameter calibration within TRNSYS. This alignment demonstrates the model's capacity to reliably reproduce the influence of key meteorological variables—such as temperature, irradiance, and wind—on energy generation. The consistency between the trends of simulated and measured data across most weeks reinforces the reliability of the model as a predictive tool for operational planning and performance evaluation.

A detailed analysis revealed that the maximum weekly relative error was 10.01%, aligning precisely with the upper threshold defined in the validation criterion, while the minimum relative error was -7.94%, reflecting occasional overestimations during certain weeks. However, over 95% of the weekly comparisons remained within the acceptable error range, demonstrating the robustness of the model even when subject to unmodeled climatic variations. These minor discrepancies are likely attributable to factors such as transient cloud cover, non-linear inverter efficiency, or slight inaccuracies in sensor measurements.

Ultimately, the validated model not only accurately reflects the current operational behavior of the solar system but also enables the simulation of future expansion scenarios, technical optimizations, and integration with emerging technologies such as energy storage and smart grids. As such, it constitutes a strategic decision-making tool for energy planning at UDES, with strong potential for replication in other institutional buildings. Furthermore, it provides a foundational framework for developing a digital energy twin, enhancing predictive maintenance and contributing to medium-term carbon footprint reduction goals.

Declaration of competing interest

"The authors declare that they have no any known financial or non-financial competing interests in any material discussed in this paper."

Acknowledgements

The authors would like to express their sincere gratitude to the Universidad de Santander (UDES) for providing detailed technical information and experimental data of the photovoltaic system installed in the Guane building.

Additionally, the authors thank the Unidades Tecnológicas de Santander (UTS) for providing access to the TRNSYS simulation tool and for the financial support granted for the publication of this research.

Author contribution

The contribution to the paper is as follows: F. Gómez: project execution, manuscript writing, model development, simulation, and analysis; B. E. Tarazona-Romero: model development, simulation, and analysis; J. G. Ascanio-Villabona: manuscript writing and results analysis; O. Palomino-Prieto: formulation of conclusions. All authors approved the final version of the manuscript.

Ethical approval statement

Ethical approval is not applicable for this research.

Informed consent

Informed consent for the publication of personal data in this article was not obtained because the study did not involve any personal data, images, or identifying information requiring such consent.

Declaration of use of AI in the writing process

The author(s) did not use any AI tools during the preparation of this work.

References

- [1] W. Murillo *et al.*, «Experimental techno-economic analysis of an autonomous photovoltaic system operating in Chocó, Colombia», *Energy Rep.*, vol. 9, pp. 258-273, sep. 2023, <https://doi.org/10.1016/j.egy.2023.05.275>.

- [2] C. Granados, M. Castañeda, S. Zapata, F. Mesa, y A. J. Aristizábal, «Feasibility analysis for the integration of solar photovoltaic technology to the Colombian residential sector through system dynamics modeling», *Energy Rep.*, vol. 8, pp. 2389-2400, nov. 2022, <https://doi.org/10.1016/j.egy.2022.01.154>.
- [3] Congreso de Colombia, «Law 1715/2014, regulating the integration and promotion of non-conventional renewable energy (FNCER) last amended by Law 2099/2021 - Climate Change Laws of the World». Accedido: 6 de abril de 2025. [En línea]. Disponible en: https://climate-laws.org/document/law-1715-2014-regulating-the-integration-and-promotion-of-non-conventional-renewable-energy-fncer_6bed
- [4] M. Haddad, N. Javani, y B. Rezaie, «Energy storage management in a near zero energy building using Li-ion, lead-acid, flywheel, and photovoltaic systems with TRNSYS simulation», *Process Saf. Environ. Prot.*, vol. 196, p. 106898, abr. 2025, <https://doi.org/10.1016/j.psep.2025.106898>.
- [5] B. E. Tarazona-Romero, N. D. Socha-Rojas, J. Ascanio-Villabona, V. Kafarov, y N. Y. Castillo-Leon, «Performance evaluation of solar thermal collectors in Colombian thermal floors by dynamic simulation», *Sustain. Eng. Innov.*, vol. 6, n.º 2, Art. n.º 2, dic. 2024, <https://doi.org/10.37868/sei.v6i2.id394>.
- [6] A. Remlaoui, D. Nehari, M. Laissaoui, y A. M. Sandid, «Performance evaluation of a solar thermal and photovoltaic hybrid system powering a direct contact membrane distillation: TRNSYS simulation», *Desalination Water Treat.*, vol. 194, pp. 37-51, ago. 2020, <https://doi.org/10.5004/dwt.2020.25834>.
- [7] F. Barrena, I. Montero, M. T. Miranda, J. I. Arranz, y F. J. Sepúlveda, «Experimental performance evaluation of self-consumption photovoltaic system with energy storage using TRNSYS», *J. Energy Storage*, vol. 92, p. 112147, jul. 2024, <https://doi.org/10.1016/j.est.2024.112147>.
- [8] A. S. Alsagri y A. A. Alrobaian, «Analysis and performance prediction of a building integrated photovoltaic thermal system with and without phase change material», *Energy*, vol. 310, p. 133249, nov. 2024, <https://doi.org/10.1016/j.energy.2024.133249>.
- [9] M. Qu, Z. Xu, X. Yan, y H. Liu, «Performance analysis of a Photovoltaic/Thermal integrated dual-source heat pump with electrical energy storage system for building heating applications», *Energy Build.*, vol. 334, p. 115526, may 2025, <https://doi.org/10.1016/j.enbuild.2025.115526>.
- [10] Chr. Lamnatou, C. Cristofari, y D. Chemisana, «Artificial Intelligence (AI) in relation to environmental life-cycle assessment, photovoltaics, smart grids and small-island economies», *Sustain. Energy Technol. Assess.*, vol. 71, p. 104005, nov. 2024, <https://doi.org/10.1016/j.seta.2024.104005>.
- [11] M. S. Saleem y N. Abas, «Optimal design of renewable driven polygeneration system: A novel approach integrating TRNSYS-GenOpt linkage», *Clean. Eng. Technol.*, vol. 24, p. 100856, feb. 2025, <https://doi.org/10.1016/j.clet.2024.100856>.
- [12] A. M. A. Alshibil, I. Farkas, y P. Víg, «Multi-aspect approach of electrical and thermal performance evaluation for hybrid photovoltaic/thermal solar collector using TRNSYS tool», *Int. J. Thermofluids*, vol. 16, p. 100222, nov. 2022, <https://doi.org/10.1016/j.ijft.2022.100222>.
- [13] B. E. Tarazona-Romero, C. L. Sandoval-Rodriguez, O. Lengerke-Pérez, J. S. Becerra-Reyes, y A. Velandia-Esparza, «Performance Evaluation of a Linear Fresnel Concentrator Applying Numerical Simulation», 2023, Accedido: 6 de abril de 2025. [En línea]. Disponible en: <https://www.scitepress.org/Papers/2022/118265/118265.pdf>
- [14] B. E. Tarazona-Romero, A. R. Arenas-Gracia, y J. C. Jaimes-Orostegui, «Performance Evaluation of a Parabolic Trough Collector Applying SolTrace and TRNSYS», 2023, Accedido: 6 de abril de 2025. [En línea]. Disponible en: <https://www.scitepress.org/Papers/2022/119597/119597.pdf>
- [15] Grupo Planeta Ambiental, «Construcción del sistema de producción de energía a partir de FNCE (fotovoltaica), 60 Wkp. Universidad de Santander – UDES, Bucaramanga, Santander.» 2017.

- [16] W. De Soto, S. A. Klein, y W. A. Beckman, «Improvement and validation of a model for photovoltaic array performance», *Sol. Energy*, vol. 80, n.º 1, pp. 78-88, ene. 2006, <https://doi.org/10.1016/j.solener.2005.06.010>.